Supplementary Information

Grammatical Evolution-based design of the SARS-CoV-2 main protease inhibitors.

Francisco Frausto-Parada[a], Ismael Várgas-Rodríguez[a], Itzel Mercado-Sánchez[a], Adán Bazán-Jiménez[a], Erik Díaz-Cervantes[b], Marco A. Sotelo-Figueroa[c]*, Marco A. García-Revilla[a]*

Covalent Docking

Table SI-1. Covalent Docking: Results of the two-point attractor method using the crystal structure 6Y2F. Values show the influence of different δ and ε on docking accuracy RMSD (Å) with respect to the experimental structure and binding free energy (kcal/mol).

	RMSD (Å)						Binding Energy (Kcal/mol)					
Width (δ)	ε-10	ε-30	ε-40	ε-50	ε-100	ε-1000	ε-10	ε-30	ε-40	ε-50	ε-100	ε-1000
1	2.37	2.18	2.52	2.47	2.30	2.32	-7.43	-7.86	-7.87	-7.50	-7.90	-7.43
3	1.62	1.64	1.74	2.15	2.43	1.90	-8.40	-7.87	-8.57	-7.00	-8.02	-8.52
5	2.13	2.23	1.61	2.14	1.91	1.95	-7.18	-6.81	-7.51	-9.65	-9.50	-8.39

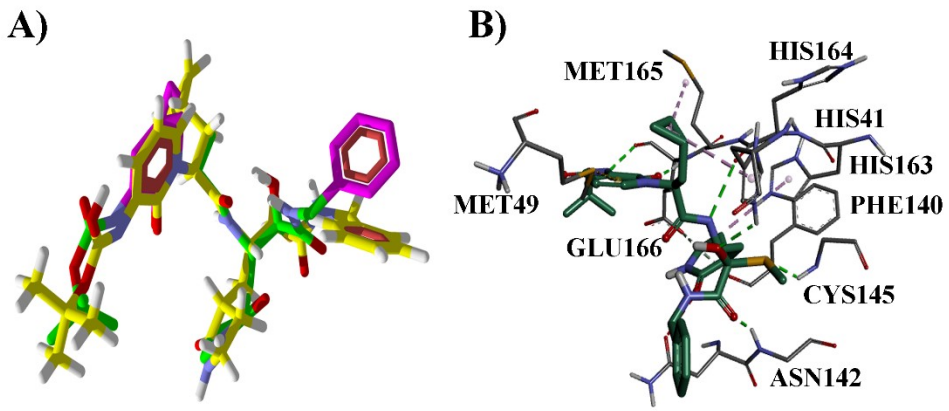

Figure SI-1. Result of covalent docking between 13b and SARS-CoV2^{pro}. A) Best pose of 13b with the covalently bound residues (green) compared with the crystallographic pose (yellow) of the ligand. B) interactions of 13b with the active site of the protein once the covalent coupling was performed with the two-point attractor method in this work.

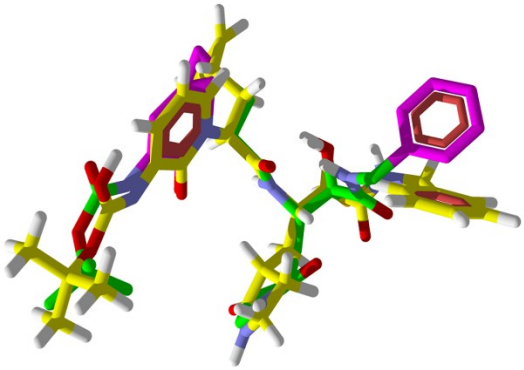

Figure SI-2. Detail of covalent docking between 13b and SARS-CoV2PRO. A) Best pose of 13b with the covalently bound residues (green) compared with the crystallographic pose (yellow) of the ligand.

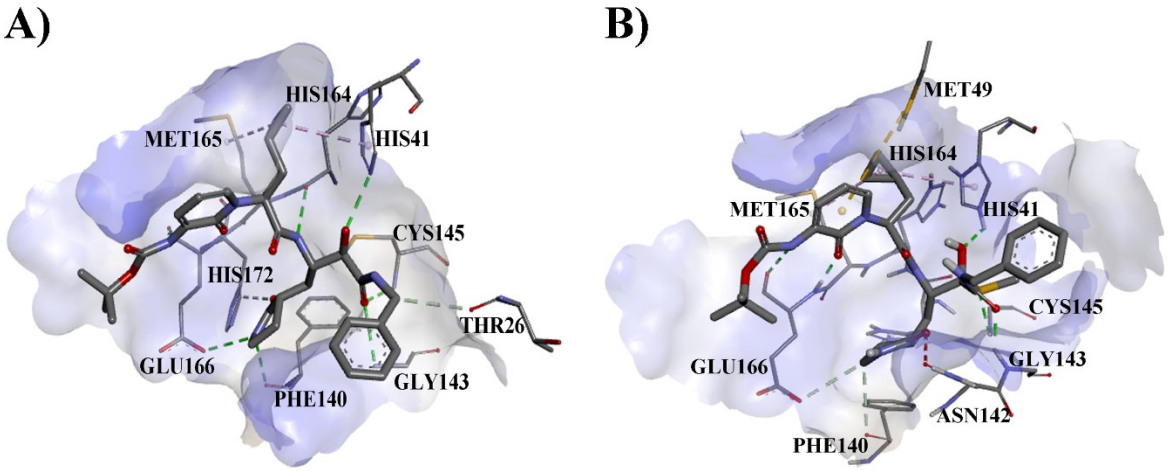

Figure SI-3. Comparation between the interactions of 13b and SARS-CoV-2-M^{pro}. A) Co-Crystallized molecule (PDB:6Y2F) and B) Covalent Docking performed in this work. Hydrogen bond is displayed as green dashed lines, alkyl interactions are displayed as dashed pink lines and pi-sigma interactions are displayed as purple line.

AutoDock Vina

Additionally, the molecular docking was performed with AutoDock Vina and we used the scoring function AutoDock Vina, [1]. AutoDock Vina differs from Autodock in the scoring function, and, in general, AutoDock Vina scoring function performs better, both in speed and accuracy [1]. The maximum number of binding modes generated was 20, the search space cartesian coordinates was (11.687, -1.471, 22.252), the number of points in x, y and x dimension was 16, 18 and 24, respectively.

We performed a docking simulation with AutoDock Vina for 13b, TSO, TBO, TTO ligands with the SARS-CoV-2- M^{pro}, Figure 1. For the calibrating docking with the reference compound 13b, we obtained a RMSD of 1.859 Å and binding energy of -5.7 Kcal/mol. For the case of new ligands, the one with higher binding energy was TBO (-7.0 Kcal/mol), followed by TSO and the ligand with the lowest binding energy was TTO, Table 1. This result agrees with the trend of results of AutoDock 4.2. Regarding the results of docking between commercial drugs (CQ, HCQ, FAV-RTP and REM-RTP) and SARS-CoV-2- M^{pro}, the binding energy was lower than 13b, TBO, TSO and TTO, nevertheless, REM-RTP displays a large interaction energy (-7.3 kcal/mol), Table SI-2.

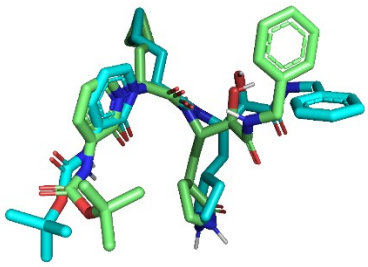

Figure SI-4. Result of docking with AutoDock Vina. The best pose of 13b (green) compared with the co-crystallized ligand (blue), RMSD of 1.859 Å.

A comparison between the best pose of results of Autodock 4.2, Covalent Docking and Autodock Vina is placed in Figure SI-5. As it can be observed all poses hold high similitude, all the functional groups are in almost the same position.

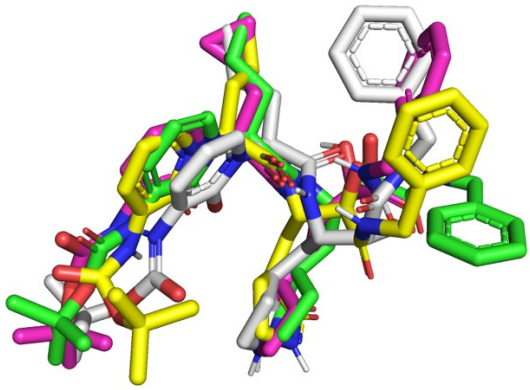

Figure SI-5. Poses obtained by all used methodologies compared. Co-crystallized structure in green, simple autodock 4.0 docking in white, covalent docking in pink and autodocking vina pose in yellow.

Table SI-2. Value of binding Energy between ligands and SARS-CoV-2-M^{pro}, in Kcal/mol.

	13b	TSO	TBO	TTO	CQ	HCQ	FAV-NTP	REM-RTP
Binding Energy	-5.7	-5.5	-7.0	-5.4	-5.2	-5.2	-6.8	-7.3

The interactions we find in the coupling of 13b with SARS-CoV-2- M^{pro} are discussed below.

We observed three hydrogen bonds with GLU^{166} and 13b, hydrogen bond interactions are observed between 13b and residues HIS^{163}, HIS^{164}, PHE^{140}, GLY^{144} and SER^{144}. Besides, TSO displays two hydrogen bonds whit SER^{144} and ASN^{142}. The ligand TBO shows hydrogen bonds in the active site with GLU^{166}, CYS^{44}, LEU^{141}, ASN^{142} and GLY^{143}. Regarding interactions of CQ, HCQ, FAV-NTP and REM-RTP, we observed that only REM-RTP shows hydrogen bonds with GLU^{166} and other residues as CYS^{44}, THR^{25}, SER^{144}, ASN^{142}, LEU^{141}, HIS^{164}, HIS^{163} and MET^{165}; unlike QC and HCQ, which had maximum of two hydrogen bond interactions, and FAV-NTP which shows a few interactions with SARS-CoV-2- M^{pro}. Therefore, the above demonstrated that the more hydrogen bonds are found in the molecular coupling the higher the binding energy, Figure 2.

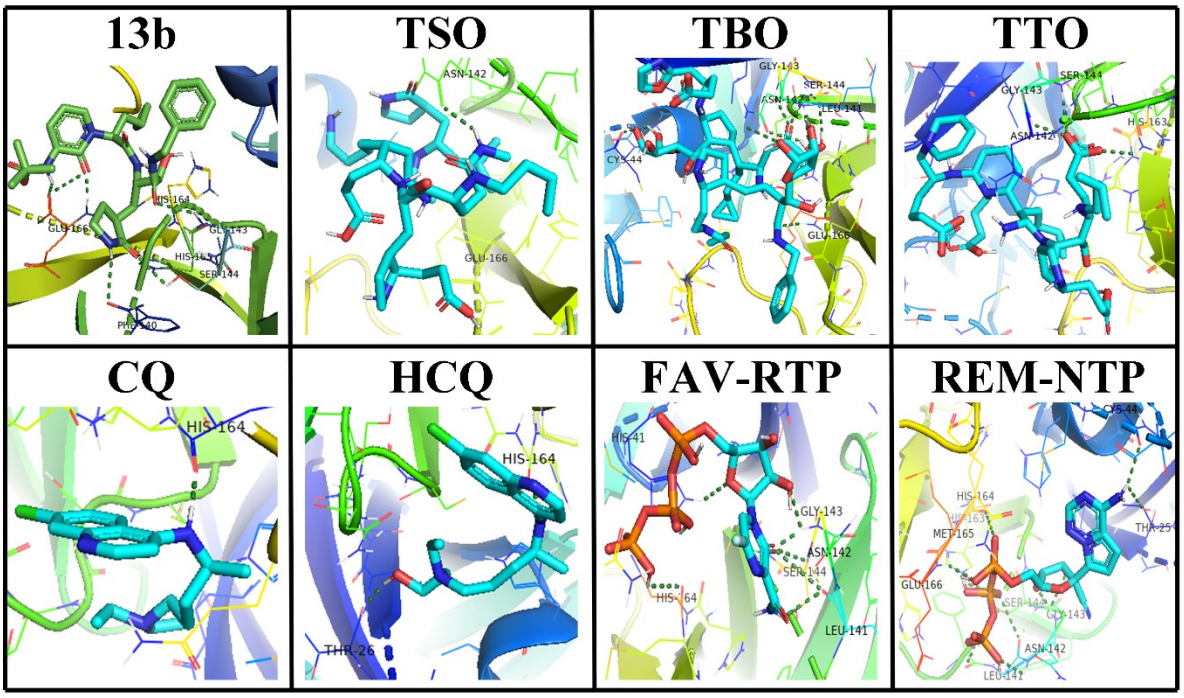

Figure SI-6. Molecular coupling of ligands in SARS-CoV-2-M^{pro}using Audotock Vina. Hydrogen bonds are displayed as green dashed lines.

1. Trott, O. and A.J. Olson, *AutoDock Vina: improving the speed and accuracy of docking with a new scoring function, efficient optimization, and multithreading.* Journal of computational chemistry, 2010. **31**(2): p. 455-461.